Biophysical Journal Volume 75 December 1998 2721–2731

Electrorheological Modeling of the Permeabilization of the Stratum Corneum: Theory and Experiment

P. Pawlowski, S. A. Gallo, P. G. Johnson, and S. W. Hui
Biophysics Department, Roswell Park Cancer Institute, Buffalo, New York 14263 USA

ABSTRACT Experimentally observed changes in the conductivity of skin under the influence of a pulsing electric field were theoretically analyzed on the basis of a proposed electrorheological model of the stratum corneum (SC). The dependence of relative changes in conductivity on the amplitude of electric field and timelike parameters of applied pulses or pulse trains have been mathematically described. Statistical characteristics of phenomena of transient and long-term electroporation of SC were taken into consideration. The time-dependent decreases of skin resistance depicted by the models were fitted to experimental data for transient and long-term skin permeabilization by electric pulses. The results show two characteristic times and two spectra of characteristic energies for transient and long-term permeabilizations. The rheological parameters derived from the fittings agreed with those reported elsewhere for biological membranes.

INTRODUCTION

The permeabilization of the skin by applying short, high voltage electrical pulses (electroporation) has great potential in enhancing drug delivery. The electrical resistance of the skin is dominated by the stratum corneum (SC), which, in its electrical property, is similar to multilamellar lipid membranes (Chizmadzhev et al., 1995). There have been a number of successful experiments to permeabilize the skin by electroporation. Several theoretical approaches to the problem of electric permeabilization of artificial or biological membranes have been reported. These studies often consider the electric polarization energy as the major factor in generating membrane pores (Sugar and Neumann, 1984; Weaver and Powell, 1989; Barnett and Weaver, 1991; Weaver, 1994). There are also a few models based on electrocompression force consideration (Chang, 1989; Crowley, 1973; Zimmermann et al., 1977, 1990; Needham and Hochmuth, 1989; Stenger et al., 1991). It becomes obvious later in this paper that, when considering time-dependent responses of electroporation, the membrane viscoelastic extensil deformation must be taken into account. Therefore, the electrocompression force approach is important.

The mechanical response of the membrane to the action of stress, as well as its quantitative characteristics, is strictly related to the rheological properties of the membrane. In an external electric field, biological membranes are subjected to different types of induced mechanical stress. The form of stress depends on the electric and geometric parameters of the system, leading to the domination of either the shear (Pawlowski and Fikus, 1991) or the extensil stress (Pawlowski and Fikus, 1993). The latter type of stress, which equals the difference between the isotropic part of mechanical stresses on the membrane surface and the stress in the direction perpendicular to the membrane, dominates in the low frequency range of oscillations. It results in the extensil deformation of the membrane, which means the change in the area of the membrane or the corresponding opposite change in its thickness without change in its volume (Needham and Hochmuth, 1989). Extensil deformation can lead to transient or permanent destabilization of the membrane, manifesting itself by electroporation or electrodestruction (Pawlowski et al., 1993).

In a recent report, electric pulses were applied to porcine skins to permeabilize them electrically (Gallo et al., 1997). It was found that, under certain conditions, the skin could be permeabilized transiently by a single pulse, or long-term permeabilization could be achieved by using a train of higher voltage pulses. In this paper we apply the viscoelastic membrane model to quantitatively describe the deformation of the SC by the applied electric pulses. We propose two parallel rheological models to describe viscoelastic deformations of the SC in an electric field. In this way we can analyze the transient (reversible) and long-term (irreversible) permeabilization of the SC by low frequency pulsing electric fields. We found that the relative change in conductivity may be described as an analytical function of the amplitude of the electric field and timelike parameters of applied pulses or pulse trains. Electroporation may then be quantitated in terms of the changes in total skin conductivity as a function of deformation, or of stress and time. The statistical nature of the permeabilization energy is revealed in the analysis of deformation with electroporation. Finally, the theoretical model is applied to interpret experimental results.

ELECTRORHEOLOGICAL MODEL OF THE STRATUM CORNEUM

In the following analysis, we first express the conductivity of the skin as a function of its extensil deformation. We then calculate the change of the

Received for publication 24 March 1997 and in final form 6 August 1998.
Address reprint requests to Dr. Sek Wen Hui, Membrane Biophysics Laboratory, Roswell Park Cancer Institute, Elm & Carlton Streets, Buffalo, NY 14263. Tel.: 716-845-8595; Fax: 716-845-8899; E-mail: roswhui@acsu.buffalo.edu.

0006-3495/98/12/2721/11 $2.00

skin conductivity as a result of the applied extensil stress that may statistically reach the range of pore-forming energy.

For simplicity, we assume that each "locally macroscopic" horizontal slice of the SC (Fig. 1) consists of a layer of nonconducting viscoelastic membranes, randomly perforated by a system of naturally occurring conducting routes (appendageal routes, natural defects of the SC), and an underlying layer of nonviscous conducting liquid.

In the absence of electropores, the electric resistance (dR_o) of such a slice of SC equals

$$dR_o = (\rho dz/S_o)[\alpha_m(S_o/S_n) + (1 - \alpha_m)], \tag{1}$$

where ρ is the specific resistivity of the conducting liquid within the conducting routes and the underlying layer, dz is the total thickness of the slice, S_o is the area of the slice, S_n is the total cross section area of naturally occurring conducting routes, and α_m is the fractional thickness of the nonconducting viscoelastic "membrane" layer in the total thickness of the slice ($\alpha_m \leq 1$).

In the case of electroporation of the membrane layer, the electric resistance (dR) of such a slice equals

$$dR = (\rho dz/S_o)\{\alpha_m[S_o/(S_n + S_p)] + 1 - \alpha_m\}, \tag{2}$$

where S_p is the total cross section area of conducting pores.

In the case when $\alpha_m \cong 1$, $S_n \ll S_o$, and $S_p \ll S_o$, Eqs. 1 and 2 can be written in the form

$$dR_o = (\rho dz/S_o)\alpha_m(S_o/S_n), \tag{3}$$

$$dR = (\rho dz/S_o)\alpha_m[S_o/(S_n + S_p)]. \tag{4}$$

Assuming that all slices of SC are electrically identical, it is possible to obtain resistivities R_o and R for the entire SC of thickness H:

$$R_o = \alpha_m(\rho H/S_n), \tag{5}$$

$$R = \alpha_m(\rho H/(S_n + S_p)]. \tag{6}$$

If we define conductivities σ_o and σ, where $\sigma_o = 1/R_o$ and $\sigma = 1/R$, by using Eqs. 5 and 6 we can write the relative increase in conductivity, (RIC), defined as

$$\mathrm{RIC} = (\sigma - \sigma_o)/\sigma_o, \tag{7}$$

which equals

$$\mathrm{RIC} = S_p/S_n. \tag{8}$$

We assume that there are two distinct types of membrane regions "f" and "s." The region of type "f" responds relatively rapidly and reversibly to stress, as depicted by the viscoelastic rheological model 1 (m.r. 1 in Fig. 2). The region of type "s" responds relatively slowly and irreversibly to the action of stress, as depicted by the viscoelastic rheological model 2 (m.r. 2 in Fig. 2). The initial, unperforated membrane area S_m ($= S_o - S_n$) in each slice can be written as a sum:

$$S_m = S_f + S_s, \tag{9}$$

where S_f and S_s are areas of the two types ("f" and "s") of membrane regions. In the case of electroporation, the total conducting area of pores can be calculated as

$$S_p = \kappa_f\, p_f S_f + \kappa_s\, p_s S_s, \tag{10}$$

where p_f and p_s are the probabilities of electroporation, and κ_f and κ_s are the ratios of characteristic time of pore closing to characteristic time of pore opening in regions "f" and "s," respectively.

The probability of electroporation in a given region can be calculated as the probability that the energy density produced by the action of the electric field exceeds a critical (enough for the formation of pore) value Δe_p. The probabilities p_f and p_s, in the "f" and "s" regions, respectively, may be expressed mathematically by calculating the integrals:

$$p_f = \int_{-\infty}^{\Delta e_f} g_f(x)dx \tag{11}$$

$$p_s = \int_{-\infty}^{\Delta e_s} g_s(x)dx \tag{12}$$

where Δe_f and Δe_s are applied energy densities due to the action of the electric field, and $g_f(x)$ and $g_s(x)$ are densities of probability that the critical value Δe_p falls in the range between x and $x + dx$ for regions "f" and "s," respectively.

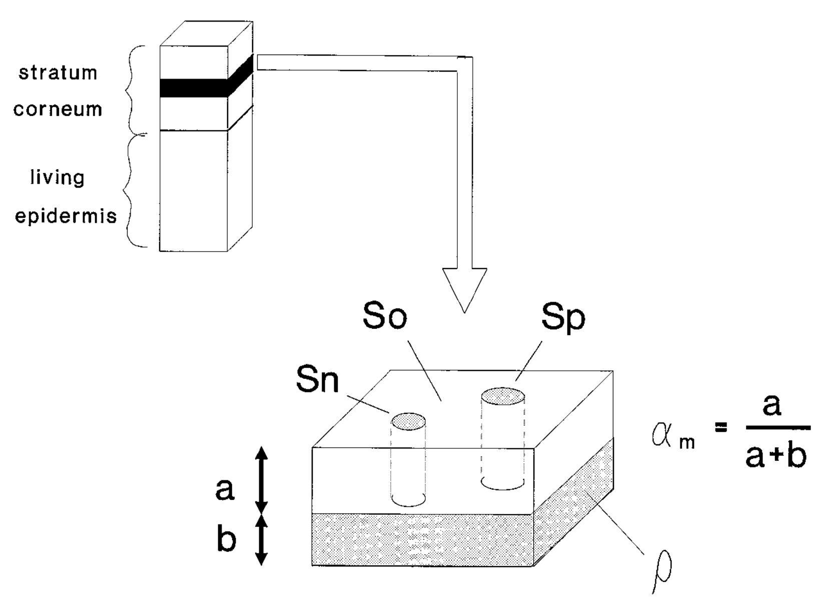

FIGURE 1 Electrorheological model of SC. The horizontal slice of the SC (*upper left*) consists of a layer of nonconducting viscoelastic membrane (*a*), randomly perforated by a system of conducting natural routes (S_n), and electrically induced pores (S_p), and a layer of conducting nonviscous liquid (*b*). The meaning of the symbols is explained in the text.

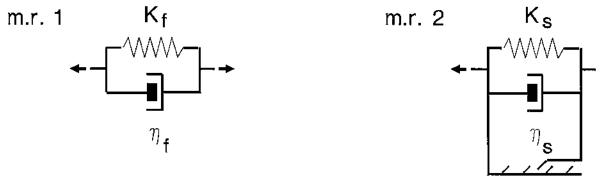

FIGURE 2 Rheological models of different membrane regions. Models m.r. 1 and m.r. 2 represent viscoelastic properties of "f" and "s" regions, respectively. Springs model elasticity, dashpots model viscosity, and the comb models irreversible response of these regions. Here K_f, K_s are area elastic moduli of the membrane and η_f, η_s are area viscosities of the membrane in regions "f" and "s" respectively.

The applied energy densities Δe_f and Δe_s can be calculated as

$$\Delta e_f = \gamma_f(\Delta S_f/S_f), \tag{13}$$

$$\Delta e_s = \gamma_s(\Delta S_s/S_s), \tag{14}$$

where γ_f and γ_s are initial tensions (in N/m^2), and $\Delta S_f/S_f$ and $\Delta S_s/S_s$ are relative increases of membrane areas caused by the action of the electric field in regions "f" and "s," respectively.

Taking into account rheological models (Fig. 2), relative increases of membrane areas during the action of pulsing electric field are described by (see Appendix 1)

$$\Delta S_f/S_f = (\tau/T)(\delta_f/K_f)\{1 - \exp[-(t/t_f)]\}, \tag{15}$$

$$\Delta S_s/S_s = (\delta_s/K_s)\{1 - \exp[-(\tau/T)(t/t_s)]\}, \tag{16}$$

where δ_f and δ_s are extensil stresses imposed on the membranes by the action of the electric field; K_f and K_s are elastic moduli of membranes (for changes in area); $t_f = \eta_f/K_f$ and $t_s = \eta_s/K_s$; η_f and η_s are viscosities in regions "f" and "s," respectively; τ is the width of a single pulse; T is the period of the pulse electric field; and t is time.

After the electric field is switched off, changes in relative area can be written as follows:

$$\Delta S_f/S_f = (\tau/T)(\delta_f/K_f)\{1 - \exp[-(t_a/t_f)]\} \exp\{-[(t - t_a)/t_f]\}, \tag{17}$$

$$\Delta S_s/S_s = (\delta_s/K_s)\{1 - \exp[-(\tau/T)(t_a/t_s)]\}, \tag{18}$$

where t_a is the cumulative time duration when the applied electric pulse train is applied to the skin.

Extensil stresses δ_f and δ_s of the membranes, caused by the action of the electric field, are described approximately by (see Appendix 2)

$$\delta_f = \epsilon_f[\Delta V_{sc}/(\alpha_m H)]^2, \tag{19}$$

$$\delta_s = \epsilon_s[\Delta V_{sc}/(\alpha_m H)]^2, \tag{20}$$

where ϵ_f and ϵ_s are dielectric permitivities for regions "f" and "s," respectively, and ΔV_{sc} is the voltage difference across the SC.

There are two cases when RIC can be expressed relatively simply. Case I is when a single pulse ($t = T$) much shorter than the characteristic response time t_s of regions of type "s" is applied. Then $p_s S_s \ll p_f S_f$ and by using Eqs. 8, 10, 11, 13, 15, 19 and the approximation that

$$\Delta V_{sc} \sim 0.5\,\Delta V, \tag{21}$$

where ΔV is the voltage difference between electrodes on the surface of the skin, it is easy to obtain, for $t = \tau$,

$$\mathrm{RIC} = \kappa_f(S_f/S_n)\int_{-\infty}^{X1} g_f(x)dx \tag{22}$$

where

$$x_1 = [(\epsilon_f\,\gamma_f)/(4K_f(\alpha_m H)^2)]\{1 - \exp[-(\tau/t_f)]\}(\Delta V)^2. \tag{23}$$

Case II is the case when a train of pulses is applied and the long-term recovery of type "s" regions is measured. Then $p_f S_f \ll p_s S_s$, and by using Eqs. 8, 10, 12, 14, 18, 20, and approximation 21 it is easy to obtain

$$\mathrm{RIC}' = \kappa_s(S_s/S_n)\int_{-\infty}^{X_{1'}} g_s(x)dx \tag{24}$$

where

$$X_{1'} = [(\epsilon_s\gamma_s)/(4K_s(\alpha_m H)^2)]\{1 - \exp[-(\tau/T)(t_a/t_s)]\}(\Delta V)^2. \tag{25}$$

RIC may be expressed as a function of applied energy Δe_f or Δe_s, which are linear terms in the Taylor approximations of functions 22 or 24 near $\Delta e_f = \langle\Delta e_p\rangle_f$ or $\Delta e_s = \langle\Delta e_p\rangle_s$, where $\langle\Delta e_p\rangle$ is mean value of Δe_p.
In case I,

$$\mathrm{RIC} = \kappa_f(S_f/S_n)\cdot\{0.5 + g_f(\langle\Delta e_p\rangle_f) \cdot[\lambda_f\{1 - \exp[-(\tau/t_f)]\}(\Delta V)^2 - \langle\Delta e_p\rangle_f]\}, \tag{26}$$

and in case II,

$$\mathrm{RIC}' = \kappa_s(S_s/S_n)\cdot\{0.5 + g_s(\langle\Delta e_p\rangle_s) \cdot[\lambda_s\{1 - \exp[-(t_a{*}/t_s)]\}(\Delta V)^2 - \langle\Delta e_p\rangle_s]\}, \tag{27}$$

where $\lambda_f = [(\epsilon_f\gamma_f)/(4K_f(\alpha_m H)^2)]$, $\lambda_s = [(\epsilon_s\gamma_s)/(4K_s(\alpha_m H)^2)]$, and $t_a^* = (\tau/T)t$ is the cumulative time of action of the electric field pulse train. Equations 26 and 27 are useful in investigations of characteristic time constants t_f and t_s.

If we define two new variables ξ and ξ' as

$$\xi = \{1 - \exp[-(\tau/t_f)]\}(\Delta V)^2, \tag{28}$$

$$\xi' = \{1 - \exp[-(t_a^*/t_s)]\}(\Delta V)^2, \tag{29}$$

differentiation of Eqs. 22 and 24 against ξ and ξ' leads to the results

$$d\,\mathrm{RIC}/d\xi = \kappa_f\,\lambda_f(S_f/S_n)g_f\{\lambda_f\xi\}, \tag{30}$$

$$d\,\mathrm{RIC}'/d\xi' = \kappa_s\,\lambda_s(S_s/S_n)g_s\{\lambda_s\xi'\}, \tag{31}$$

Equations 30 and 31 can be useful in investigations of densities of probability g_f and g_s.

RESULTS

For this study, the experimental data were taken from the work of Gallo et al. (1997). The set-up and procedure used in electroporation of porcine skin experiments were also described in that paper.

Case I

"Single pulse" experiments. Equation 26 suggests that, if the variation of the applied pulse voltage during the experiment is neglected, the trend of changes of RIC with pulse length τ has the form

$$\mathrm{RIC} = a + b\{1 - \exp[-(\tau/t_f)]\}, \quad (32)$$

where

$$a = \kappa_f(S_f/S_n)\{0.5 - g_f(\langle\Delta e_p\rangle_f)\langle\Delta e_p\rangle_f\}, \quad (33)$$

$$b = \kappa_f(S_f/S_n)g_f(\langle\Delta e_p\rangle_f)\lambda_f\langle(\Delta V)^2\rangle, \quad (34)$$

and $\langle(\Delta V)^2\rangle$ is the mean value of the square of the applied voltage difference.

Equation 32 was preliminarily fitted (see for example, Fig. 3) to the τ-dependence of experimental results taken from 21 independent measurements, classified into four groups by the voltages used (0–30, 30–60, 60–80, 110–160 V). Because all preliminary fittings showed that parameter a did not differ significantly from zero, it was assumed that $a = 0$ in the final fittings. Then the final values of $t_f =$ 1.66, 1.66, 1.85, and 1.74 ms were obtained. For future calculation the mean value of $t_f = 1.7$ ms is taken.

In the next step, RIC results were plotted against the variable ξ (Fig. 4 *A*) and differentiated. Differentiation was performed by using the linear regression method applied in the sequential neighborhoods of five to nine experimental points. In this way mean values of ξ and RIC for these neighborhoods were also obtained (Fig. 4 *B*). Finally, coefficients of slope versus mean values ξ in neighborhoods were analyzed (Fig. 4 *C*, *points*).

In the final analysis, the line shape of g_f in Eq. 30 was assumed to have the form of

$$g_f(x) = [1/(2\pi\sigma_f^2)^{1/2}]\exp\{-(x - \langle\Delta e_p\rangle_f)^2/(2\sigma_f^2)\}. \quad (35)$$

Equation 30 was fitted to differentials of RIC (Fig. 4 *C*, *continuous line)*. Before evaluation, Eq. 30 was transformed into the form

$$d\,\mathrm{RIC}/d\xi = \kappa_f(S_f/S_n)[1/(2\pi\beta_f^2)^{1/2}]\exp\{-(\xi - \langle\xi_p\rangle_f)^2/(2\beta_f^2)\}, \quad (36)$$

where

$$\langle\xi_p\rangle_f = \langle\Delta e_p\rangle_f/\lambda_f, \quad (37)$$

$$\beta_f = \sigma_f/\lambda_f. \quad (38)$$

Then $\langle\xi_p\rangle_f = 976.42 \pm 0.08\ \mathrm{V}^2$, $b_f = 500\ \mathrm{V}^2$, and $\kappa_f(S_f/S_n) = 4$ were obtained. The values of the last two parameters have no documented statistical significance.

Case II

"Pulse train" experiments. Equation 27 suggests that if we neglect the variation of applied voltage during experiments, the trend of changes of RIC′ with time t_a^* has the form

$$\mathrm{RIC}' = a' + b'\{1 - \exp[-(t_a^*/t_s)]\}, \quad (39)$$

where

$$a' = \kappa_s(S_s/S_n)\{0.5 - g_s(\langle\Delta e_p\rangle_s)\langle\Delta e_p\rangle_s\}, \quad (40)$$

$$b' = \kappa_s(S_s/S_n)g_s(\langle\Delta e_p\rangle_s)\lambda_s\langle(\Delta V)^2\rangle. \quad (41)$$

Similarly to case I, Eq. 39 was preliminarily fitted (see, for example, Fig. 5) to the t_a^*-dependence of experimental results taken from 48 independent measurements, classified into five groups by the voltages used (90–130, 170–200, 220–250, 260–300, 300–340 V). As computer fittings showed, the parameter a' did not differ significantly from zero. Therefore, it was assumed that $a' = 0$ in final fittings. The final values of $t_s = 11.8$, 7.1, 3.9, 6.5, and 7.4 s were

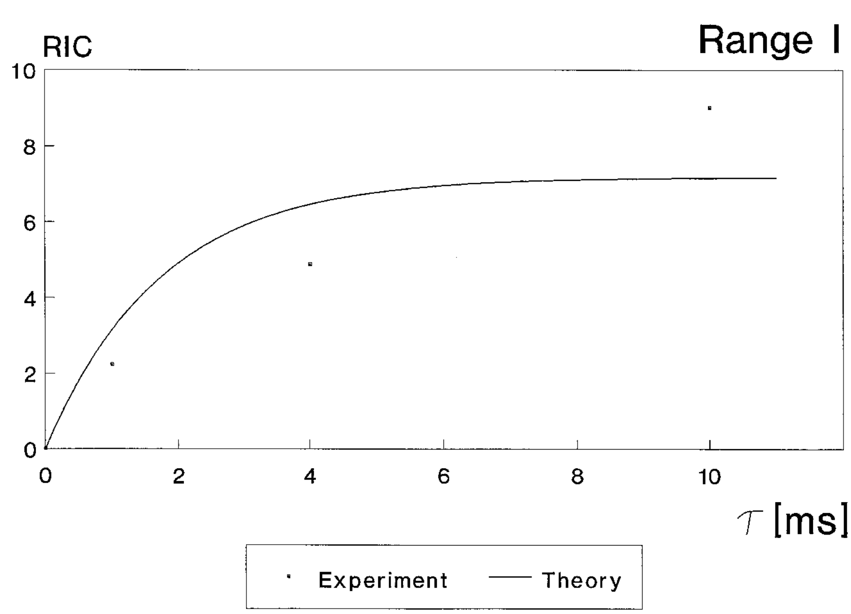

FIGURE 3 Example of a preliminary fitting of the dependence of RIC on τ for case I: single pulse experiments. Equation 32 (*solid line*) is fitted to three experimental measurements of RIC in the 110–160 V range. RIC is the relative increase in conductivity.

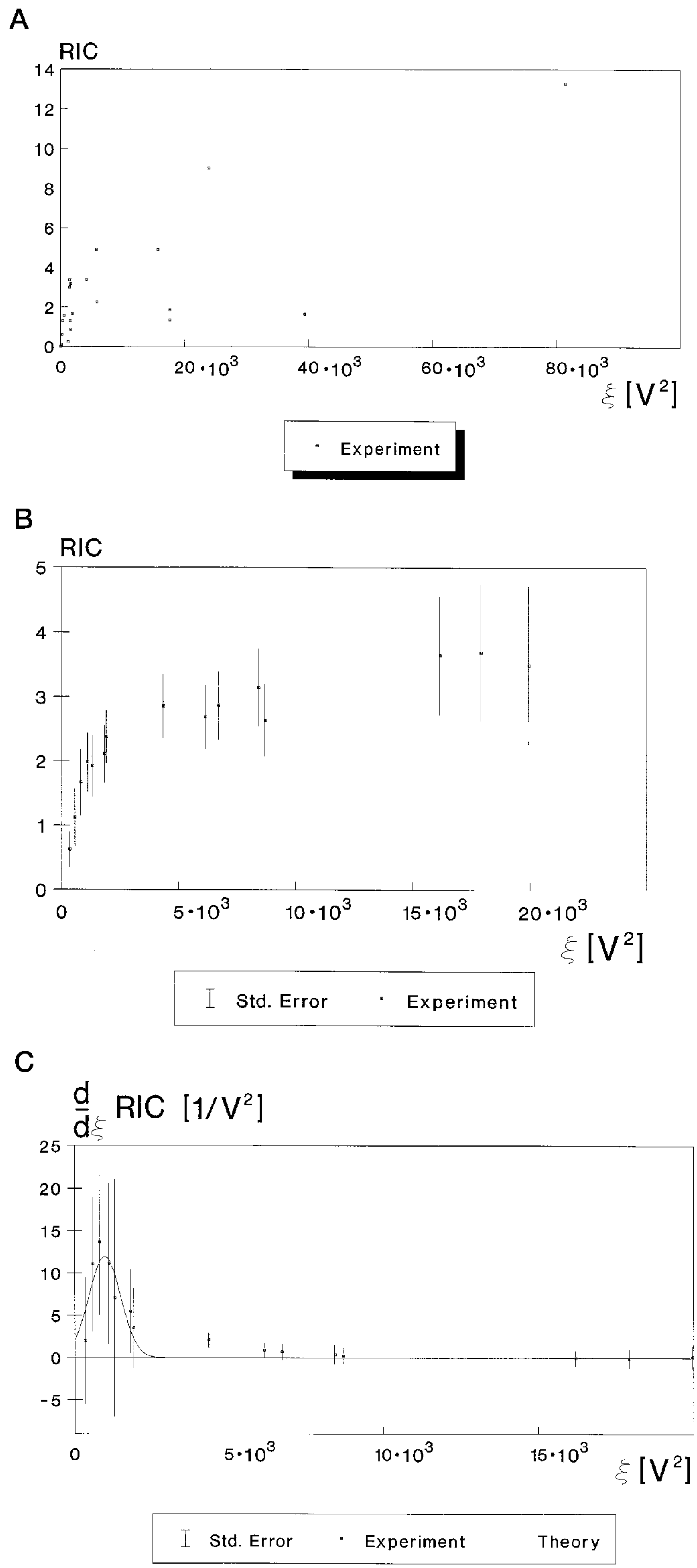

FIGURE 4 Statistical treatment of experimental data for case I: single pulse experiments. The variable ξ is defined by Eq. 28. The solid line is the fitting of Eq. 36. (*A*) Dependence of RIC on ξ; (*B*) dependence of RIC on ξ (averaged values); (*c*) dependence of differentiated RIC on ξ.

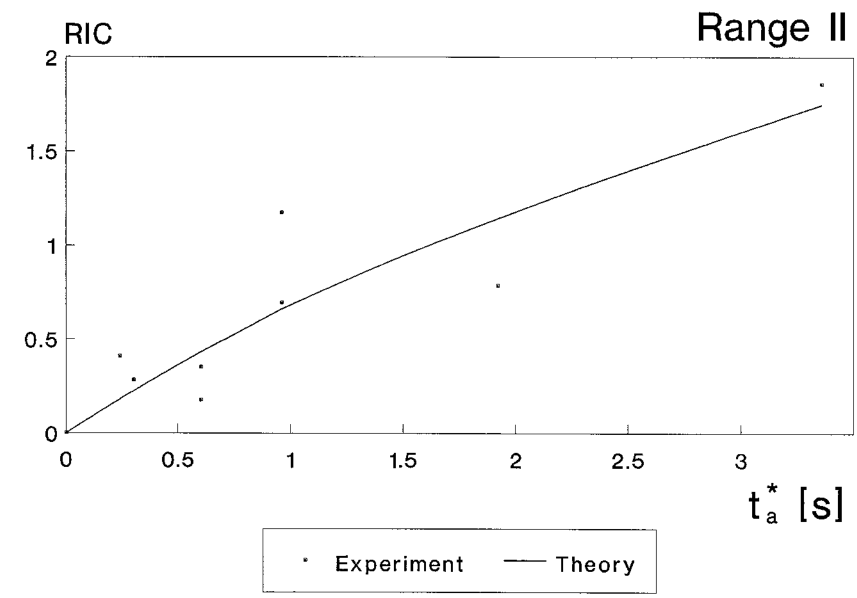

FIGURE 5 Example of a preliminary fitting of the dependence of RIC′ on t_a* for case II: "pulse train" experiments. Equation 39 (*solid line*) is fitted to eight experimental measurements of RIC′ in the 220–250 V range. RIC′ is the relative increase in conductivity.

obtained. For future calculations, the mean value of $t_s = 7$ s is taken. In the next steps, the RIC′ results were plotted against the variable ξ' (Fig. 6 *A*) and differentiated. The differentiation procedure was the same as in case I. Mean values of ξ' and RIC′ for these neighborhoods were obtained (Fig. 6 *B*). Finally, coefficients of slope versus mean values of ξ' in neighborhoods were analyzed (Fig. 6 *C*, *points*).

In the final analysis, the function g_s in Eq. 31 was assumed to have the form

$$g_s(x) = [1/(2\pi\sigma_s^2)^{1/2}]\exp\{-(x - \langle\Delta e_p\rangle_s)^2/(2\sigma_s^2)\} + g_{so}. \tag{42}$$

Equation 31 was fitted to differentials of RIC′ (Fig. 6 *C*, *continuous line*). Before evaluation, Eq. 31 was transformed into the form

$$d\mathrm{RIC}'/d\xi' = \kappa_s(S_s/S_n)[1/(2\pi\beta_s^2)^{1/2}] \exp\{-(\xi - \langle\xi_p\rangle_s)^2/(2\beta_s^2)\} + e_s, \tag{43}$$

where

$$\langle\xi_p\rangle_s = \langle\Delta e_p\rangle_s/\lambda_s, \tag{44}$$

$$\beta_s = \sigma_s/\lambda_s, \tag{45}$$

$$e_s = \kappa_s(S_s/S_n)\lambda_s\, g_{so}. \tag{46}$$

Then $\langle\xi_p\rangle_s = 49802.886 \pm 0.014$ V^2, $\beta_s = (629 \pm 25)*10^1$ V^2, $\kappa_s(S_s/S_n) = 1.41 \pm 0.06$, and $e_s = (8.964 \pm 0.001)*10^{-6}$ V^{-2} were obtained.

DISCUSSION

In most theoretical considerations of electroporation (see Introduction) mechanical forces generated by the pulse field and their relationship to membrane deformation are often overlooked. Neglecting this information can lead to incorrect analysis. Let us consider the energy of a flat piece of membrane before pore formation. Increase of mechanical energy related with its lateral extension in an electric field can be calculated as $\Delta e = (\gamma/K)\epsilon_m E_m{}^2$V, where γ is the initial tension, K is the area elasticity, ϵ_m is the membrane dielectric permitivity, E_m is the electric field in the membrane, and V is the volume of the membrane piece. The increase of polarization energy can be written in the form $\Delta e' = (1/2)(\epsilon_m - \epsilon_o)E_m{}^2$V where ϵ_o is a dielectric permitivity of the vacuum. Since γ (in reality equal to twice the surface tension divided by the membrane thickness) is usually close to K (Evans and Skalak, 1980) and $\epsilon_m - \epsilon_o$ differs little from ϵ_m, Δe is twice the $\Delta e'$. It is obvious that energy of extensil deformation cannot be omitted from energetic considerations. This is why the present analysis concentrates on extensil deformation. Up to now only the ideal elastic deformation has been considered in the proposed electrocompression models of electroporation. The reason is that the viscosity for area changes in cellular or artificial membranes is very small (Evans and Hochmuth, 1978). However, if short time impulses or "fatigued" membrane with the increased viscosity is considered, the viscosity contribution could be significant (adequate characteristic times could be measurable). Keeping the above remark in mind, we include viscosity into our theoretical consideration.

By using the results of our analysis of experimental data, it is possible to estimate values of many important physical parameters of the stratum corneum. By assuming that the SC contains in its entire thickness ~100 membranes (that means putting $\alpha_m H = 10^{-6}$ m) and by taking $\epsilon_f = \epsilon_s = 10^{-10}$ F/m, $\gamma_f = K_f$, $\gamma_s = K_s$ (Pawlowski et al., 1993) and using Eqs. 37 and 44, one may obtain $\langle\Delta e_p\rangle_f = 3 \cdot 10^4$ J/m^3 and $\langle\Delta e_p\rangle_s = 3 \cdot 10^4$ J/m^3. These values of average critical energy density are close to those obtained with a different

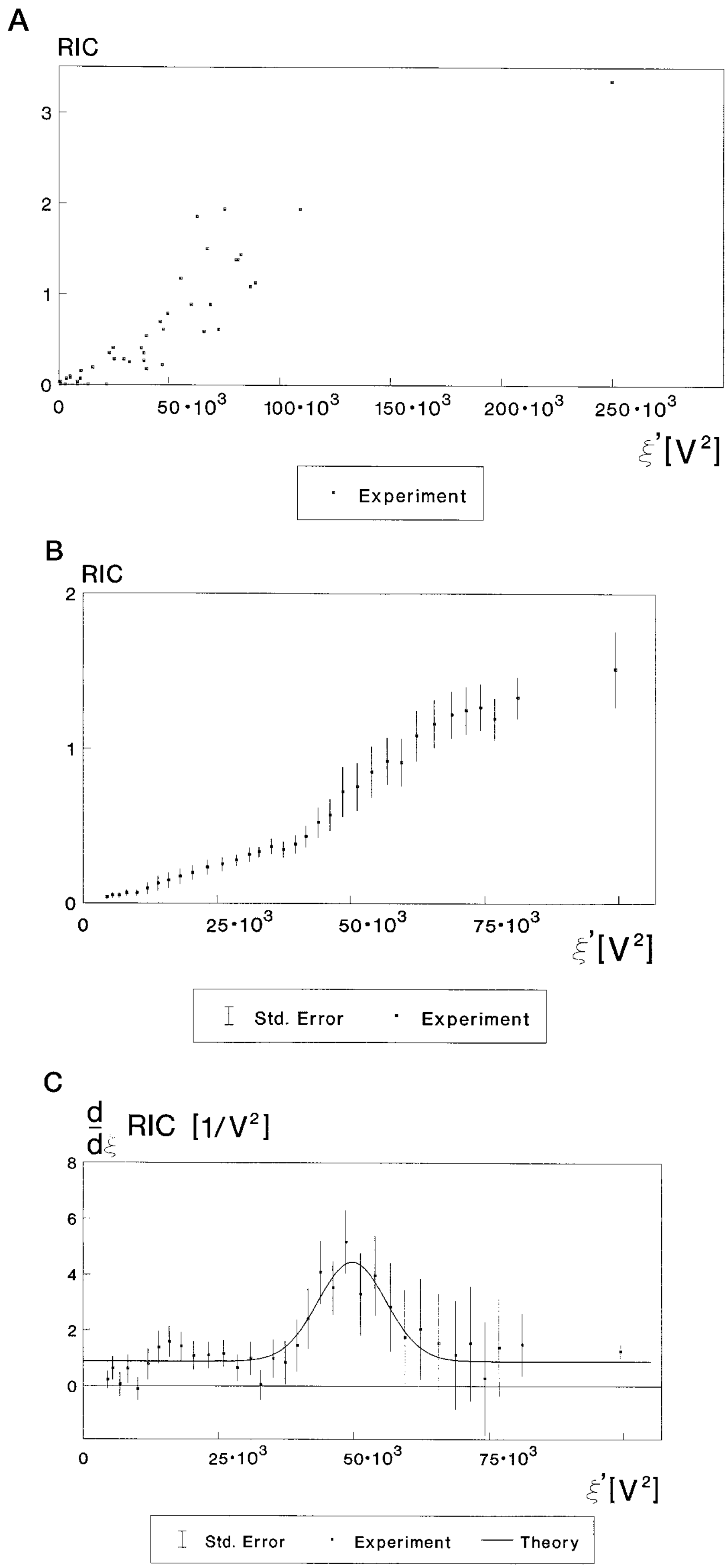

FIGURE 6 Statistical treatment of experimental data for case II: "pulse train" experiments. The variable ξ' is defined by Eq. 29. Solid line is the fitting of Eq. 43. (*A*) Dependence of RIC′ on ξ'; (*B*) dependence of RIC′ on ξ' (averaged values); (*C*) dependence of differentiated RIC′ on ξ'.

method for membranes of single cells (Pawlowski et al., 1996). Such results suggest that the proposed electrorheological model deserves further investigation. It also shows that the mean value of energy for irreversible permeabilization is one order of magnitude higher than that of energy for reversible permeabilization. With the above assumptions and estimations, Eqs. 35, 37, 38, 42, and 44–46 give quantitative and graphical (Fig. 7) descriptions of the full spectrum of critical energies. The difference between mean values (in Gaussian profiles) of critical energies for electroporation in regions "f" and "s" is statistically significant. The constant component g_{so} in the function of density of probability (Eq. 42) suggests a subpopulation in the regions of type "s" that is characterized by a relatively wide range of critical energies. It is an open question how significant is the contribution of sample-to-sample variability to standard deviations of proposed Gaussian distributions. In other words, how broad the biological divergence is.

Taking $K_f = K_s = 10^6$ N/m^2 (Pawlowski et al., 1993) and definitions under Eqs. 15 and 16, it is simple to calculate that regional viscosities $\eta_f = 2 \cdot 10^3$ Ns/m^2 and $\eta_s = 7 \cdot 10^6$ Ns/m^2. The value of η_f is close to the value 10^2 Ns/m^2 reported earlier for erythrocytes (Paulitschke and Nash, 1993), and the value of η_s is close to 10^5 Ns/m^2, which was obtained for long-term stretching of *N. crassa* membrane (Pawlowski et al., 1997).

The analysis also yields the weighted areas of regions $\kappa_f S_f + \kappa_s S_s \cong 5\ S_n$. It means that if the other areas do not respond to the electric field, $\kappa_f = \kappa_s$, and the area of natural routes $S_n = (1/100)S_o$, then κ_f and κ_s equal 0.05. It means that, with these assumptions, our results show that pores should close faster than they open. To remove that open/close time asymmetry, S_n would have to be 17% of S_o.

According to Eq. 39, in case II, for the same value of t_a^*, values of RIC′ should be the same if other parameters of analysis are kept constant. In general, the values of rheological parameters (K_s, η_s) of membranes may depend on the dynamics of stretching and may change with pulse frequency $f = 1/T$ (Barnes et al., 1989). For example, the elasticity K_s may increase and/or the viscosity η_s may decrease with increasing frequency. It can cause decrease of the value of t_s. At the first approximation, we may assume that $t_a^*/t_s = (t_a^*/t_s(0)) + \chi f$, where $t_s(0)$ is the value of t_s at $f = 0$, and χ is the linear coefficient of the Taylor expansion of t_s around $f = 0$. With the above assumption, Eq. 39 was used to analyze results of frequency dependence of RIC′ (Fig. 8). By fitting of the modified Eq. 39 as a function of frequency, the values of $a' = 0$ (preliminary fitting), $b' = 2.784 \pm 0.204$, $t_a^*/t_s(0) = 0.2$ (estimated by using $t_a^* = 1.25$ s, $t_s = 7$ s), and $\chi = 0.029$ s were obtained. The last value has no statistical significance. It is difficult to discuss these results because there are no known data available, but it will not be difficult to extend the present analysis when there are more time-dependent data of the electroporation of the stratum corneum available in the future.

APPENDIX 1

In the "f"-type region, characterized by parameters of the Voight-Kelvin rheological model (m.r. 1, Fig. 2), the relative increase of area of the membrane caused by the action of the electric field is described by the equation

$$\Delta S_f/S_f = (1/K_f)\int_{-\infty}^{t} \{1 - \exp[-((t - \zeta)/t_f)]\}(df_f/d\zeta)d\zeta, \tag{A1}$$

where f_f is a function describing the evolution of the extensil stresses caused by the action of electric field in the "f"-type membrane, ζ is a time variable, t_f is the retardation time of region "f," and $d/d\zeta$ is symbol for

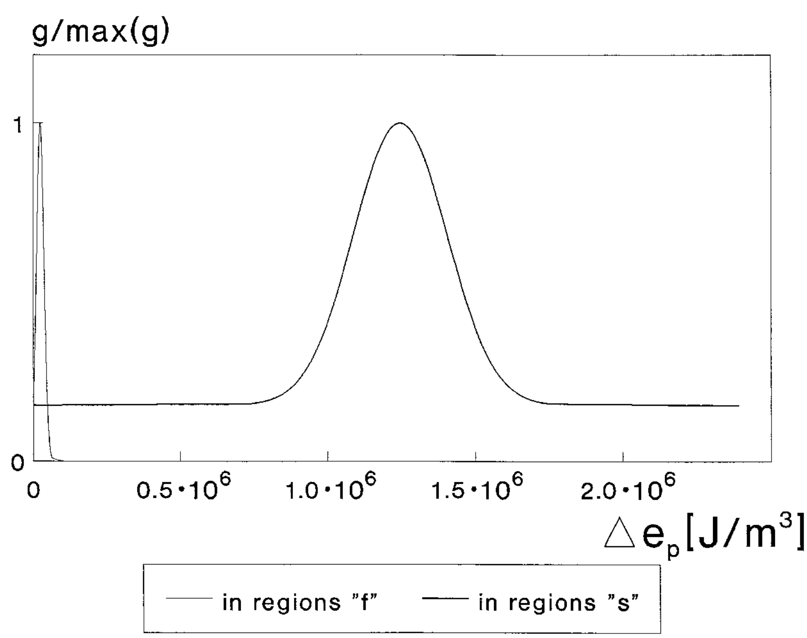

FIGURE 7 Spectrum of obtained values of critical energies for electroporation in regions of type "f" and "s," respectively. g is the density of probability, max(g) is the maximal value of g in a given distribution, and Δe_p is the critical energy of electroporation. Solid lines are obtained from transformation of lines in Figs. 4 *C* and 6 *C*.

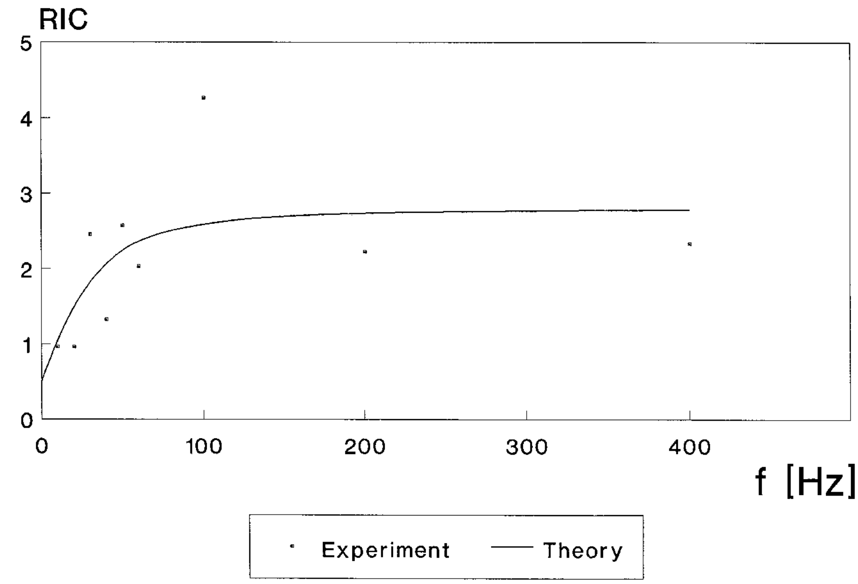

FIGURE 8 Dependence of RIC′ on frequency. RIC′ is the relative increase in conductivity, f is the pulse frequency.

differential,

$$f_f = \delta_f\left(\sum_{i=0}^{N}\{\Theta[\zeta - iT] - \Theta[\zeta - (iT + \tau)]\}\right), \quad \text{(A2)}$$

where δ_f is the amplitude of extensil stress in the region "f," Θ is the Heaviside theta function, and $NT + \tau \leq t$.

When putting into Eq. A1, it is easy to obtain

$$\Delta S_f/S_f = (\delta_f/K_f)\int_{-\infty}^{t}\{1 - \exp[-((t-\zeta)/t_f)]\} \cdot \left\{\sum_{i=0}^{N}\{\delta[\zeta - iT] - \delta[\zeta - (iT + \tau)]\}\right\}d\zeta, \quad \text{(A3)}$$

where δ is the Dirac delta function.

Integrating formula A3 leads to the equation

$$\Delta S_f/S_f = (\delta_f/K_f) \cdot \left(\sum_{i=0}^{N}\{\exp[-((t - iT - \tau)/t_f)] - \exp[-((t - iT)/t_f)]\}\right), \quad \text{(A4)}$$

which can be rewritten in the form

$$\Delta S_f/S_f = (\delta_f/K_f)\{\exp[-((t-\tau)/t_f)] - \exp[-(t/t_f)]\}\sum_{i=0}^{N}\exp(iT/t_f). \quad \text{(A5)}$$

By calculation of the sum of the geometric series in Eq. A5 one can obtain

$$(\Delta S_f/S_f = (\delta_f/K_f)\{\exp[-((t-\tau)/t_f)] - \exp[-(t/t_f)]\} \cdot \{\{1 - \exp[(N+1)T/t_f]\}/\{1 - \exp(T/t_f)\}\}. \quad \text{(A6)}$$

At any moment of observation $t = NT + \tau$, it is easy to show that

$$\Delta S_f/S_f = (\delta_f/K_f)\{\{1 - \exp(\tau/t_f)\}/\{1 - \exp(T/t_f)\}\} \exp[(T-\tau)/t_f)]\{1 - \exp[-((t + T - \tau)/T_f)]\}. \quad \text{(A7)}$$

The above general equation, in the case when $\tau \cong T \ll t \cong t_f$, can be written in the form

$$\Delta S_f/S_f = (\delta_f/K_f)(\tau/T)\{1 - \exp[-(t/t_f)]\}. \quad \text{(A8)}$$

In the case of one pulse, $\tau = T$ and $t = \tau$, Eq. A7 can be simplified to the well-known form

$$\Delta S_f/S_f = (\delta_f/K_f)\{1 - \exp[-(\tau/t_f)]\}. \quad \text{(A9)}$$

In the "s"-type region, characterized by parameters of the Voight-Kelvin rheological model with an "asymmetric comb" (m.r. 2, Fig. 2), the relative increase of area of the membrane caused by the action of the electric field is described by the equation

$$\Delta S_s/S_s = (1/K_s)\int_{-\infty}^{t}\{1 - \exp[-((t - \zeta - \mathbf{t})/t_s)]\}(df_s/d\zeta)d\zeta, \quad \text{(A10)}$$

where f_s is a function describing the evolution of the extensil stresses caused by the action of electric field in the "s"-type membrane, t_s is the retardation time of region "s," and $\mathbf{t}$ is a parameter describing time with "frozen" changes in area due to the blocker.

When substituting f_s in Eq. A10 by

$$f_s = \delta_s\left(\sum_{i=0}^{N}\{\Theta[\zeta - iT] - \Theta[\zeta - (iT + \tau)]\}\right), \quad \text{(A11)}$$

where δ_s is the amplitude of extensil stress in the region "s," and by putting $t = NT + \tau$, and calculating $\mathbf{t}$ as $\mathbf{t} = (N - i)(T - \tau)$ for pulses corresponding to the index i, one can obtain

$$\Delta S_s/S_s = (\delta_s/K_s)\left(\sum_{i=0}^{N}\{\exp[-((N-i)\tau/t_s)] - \exp[-((N+1-i)\tau/t_s))\}\right). \quad (A12)$$

The summation in Eq. A12 leads to the result

$$\Delta S_s/S_s = (\delta_s/K_s)\{1 - \exp[-(N+1)\tau/t_s]\}. \quad (A13)$$

By using the $t = N + 1$ variable, the above equation can be written in the form

$$\Delta S_s/S_s = (\delta_s/K_s)\{1 - \exp[-(((t-\tau)/T) + 1)\tau/t_s]\}. \quad (A14)$$

Now assuming that $t \gg \tau$ and $t \gg T$, Eq. A14 may be written as

$$\Delta S_s/S_s = (\delta_s/K_s)\{1 - \exp[-(t\tau)/(Tt_s)]\}. \quad (A15)$$

APPENDIX 2

When estimating the increase in mechanical stress when an external electric field is applied perpendicular to the surface of a flat, nonconducting and volumetrically noncompressible dielectric membrane immersed in conducting liquid, one can use balance equations as follows:

$$T_{zz}+M_{zz} = 0, \quad (A16)$$

$$T_{xx}+M_{xx} = 0, \quad (A17)$$

$$T_{yy}+M_{yy} = 0, \quad (A18)$$

where T_{ij} are components of mechanical stress tensor in the membrane, M_{ij} are components of Maxwell stress tensor in the membrane, z is the coordinate in the direction of the applied field, and x and y are coordinates in directions perpendicular to applied electric field.

Components of the Maxwell stress tensor can be calculated by using the formula

$$M_{ij} = \epsilon(2E_iE_j - E^2\delta_{ij})/2, \quad (A19)$$

where ϵ is dielectric permitivity of the medium, E is the magnitude of the electric field in the medium, and δ_{ij} is the Kronecker delta.

Simple calculation shows that

$$M_{zz} = \epsilon_m E_m^2/2, \quad (A20)$$

$$M_{xx} = -\epsilon_m E_m^2/2, \quad (A21)$$

$$M_{yy} = M_{xx}, \quad (A22)$$

where the subscript m means in the membrane (in general in the region "f" or "s").

Equations A16–A18 and A20–A22 lead to the expressions below:

$$T_{zz} = -\epsilon_m E_m^2/2, \quad (A23)$$

$$T_{xx} = \epsilon_m E_m^2/2, \quad (A24)$$

$$T_{yy} = T_{xx}. \quad (A25)$$

The extensil stress δ_m, defined as

$$\delta_m = (T_{xx}+T_{yy})/2 - T_{zz}, \quad (A26)$$

can be written as

$$\delta_m = \epsilon_m E_m{}^2. \quad (A27)$$

When putting

$$E_m = \Delta V_{sc}/(\alpha_m H), \quad (A28)$$

where ΔV_{sc} is the voltage difference across SC and $\alpha_m H$ is the total thickness of the membrane in the direction of electric field, one can obtain

$$\delta_m = \epsilon_m[\Delta V_{sc}/(\alpha_m H)]^2. \quad (A29)$$

This work was supported by Grant GM55864 from the National Institutes of Health.

REFERENCES

Barnes, H. A., J. F. Hutton, and K. Walters. 1989. What is rheology? *In* An Introduction to Rheology, Rheology Series. K. Walters, editor. Elsevier, Amsterdam-Oxford-New York-Tokyo.

Barnett, A., and J. C. Weaver. 1991. Electroporation: a unified, quantitative theory of reversible electrical breakdown and mechanical rupture in artificial planar bilayer membranes. *Bioelectrochem. Bioelectroenerg.* 25:163–182.

Chang, D. C. 1989. Cell poration and cell fusion using an oscillating electric field. *In* Electroporation and Electrofusion in Cell Biology. E. Neumann, A. E. Sowers, C. A. Jordan, editors. Plenum Publishing Corporation, New York. 215–227.

Chizmadzhev, Y. A., V. G. Zarnitsin, J. C. Weaver, and R. O. Potts. 1995. Mechanism of electroinduced ionic species transport through a multilamellar lipid system. *Biophys. J.* 68:749–765.

Crowley, J. M. 1973. Electrical breakdown of bimolecular lipid membranes as an electromechanical instability. *Biophys. J.* 413:1711–1724.

Evans, E. A., and R. M. Hochmuth. 1978. Mechanochemical properties of membranes. *In* Current Topics in Membranes and Transport. F. Bronner and A. Kleinzeller, editors. Academic Press, New York-San Francisco-London. 410:11–64.

Evans, E. A., and R. Skalak. 1980. Mechanics and Thermodynamics of Biomembranes. CRC Press, Inc., Boca Raton, FL.

Gallo, S. A., P. G. Johnson, A. R. Oseroff, and S. W. Hui. 1997. Characterization of electric-pulse-induced permeabilization of porcine skin using surface electrodes. *Biophys. J.* 72:2805–2811.

Needham, D., and R. M. Hochmuth. 1989. Electromechanical permeabilization of lipid vesicles. Role of membrane tension and compressibility. *Biophys. J.* 455:1001–1009.

Paulitschke, M., and G. B. Nash. 1993. Micropipette methods for analysing blood cell rheology and their application to clinic research. *Clinical Hemorheology* 13:407–434.

Pawlowski, P., Poznanska, A., and Fikus, M. 1997. Bioelectrorheological model of the cell. T. Cellular deformation in the presence of cytochalasin B. *Biorheology*. 34:171–93.

Pawlowski, P., and M. Fikus. 1991. Shear deformation of the spherical shell acted on by an external alternating electric field: possible applications to cell deformation experiments. *Z. Naturforsch.* 146*c*:487–494.

Pawlowski, P., and M. Fikus. 1993. Bioelectrorheological model of the cell. 4. Analysis of the extensil deformation of the membrane in an alternating electric field. *Biophys. J.* 165:535–540.

Pawlowski, P., Poznanska, A., and Fikus, M. 1997. Bioelectrorheological model of the cell. 7. Cellular deformation in the presence of cytochalasin B. *Biorheology*. 34:171–93.

Pawlowski, P., I. Szutowicz, P. Marszalek, and M. Fikus. 1993. Bioelectrorheological model of the cell. 5. Electrodestruction of cellular membrane in alternating electric field. *Biophys. J.* 165:541–549.

Pawlowski, P., I. Szutowicz, S. Rozycki, J. Zielinski, and M. Fikus. 1996. Bioelectrorheological model of the cell. 6. Experimental verification of the rheological model of cytoplasmic membrane. *Biophys. J.* 170: 1024–1026.

Stenger, D. A., K. V. I. S. Kaler, and S. W. Hui. 1991. Dipole interactions in electrofusion: contributions of membrane potential and effective dipole to interaction pressure. *Biophys. J.* 59:1074–1084.

Sugar, I. P., and E. Neumann. 1984. Stochastic model for electric field-induced membrane pores: electroporation. *Biophys. Chem.* 19:211–225.

Weaver, J. C., and K. T. Powell. 1989. Theory of electroporation. *In* Electroporation and Electrofusion in Cell Biology. E. Neumann, A. E. Sowers, C. A. Jordan, editors. Plenum Publishing Corporation, New York. 111–126.

Weaver, J. C. 1994. Molecular basis for cell membrane electroporation. *In* A Multidisciplinary Approach to Therapy, Prevention and Rehabilitation. Vol. 720 of the Annals of the New York Academy of Sciences. 141–152.

Zimmermann, U., F. Beckers, and M. G. L. Coster. 1977. The effects of pressure on the electrical breakdown in the membranes of Valonia utricularis. *Biochim. Biophys. Acta* 4464:1339–1416.

Zimmermann, U., G. Pilwat, A. Pequeux, and R. Gilles. 1990. Electromechanical properties of human erythrocyte membranes: the pressure dependence of potassium permeability. *J. Membr. Biol.* 454: 1103–1113.